Eur. Phys. J. B **9**, 123–136 (1999)

THE EUROPEAN PHYSICAL JOURNAL B

EDP Sciences

Softening of the interactions between surfactant bilayers in a lamellar phase due to the presence of a polymer

E. Freyssingeas[1,a], D. Antelmi[1,b], P. Kékicheff[1,c], P. Richetti[2,d], and A.-M. Bellocq[2]

[1] Department of Applied Mathematics, Research School of Physical Sciences and Engineering, Australian National University, Canberra, A.C.T. 0200, Australia
[2] Centre de Recherche Paul Pascal - CNRS, Avenue A. Schweitzer, 33600 Pessac, France

Received 2 February 1998

Abstract. The compressibility modulus of a lamellar phase containing a neutral polymer guest molecule was measured directly using a surface force apparatus. The system studied consisted of sodium dodecyl sulphate (SDS), pentanol, water and polyethylene glycol (PEG) (M_w = 22 600 g/mol). The lamellar phase was induced from a micellar phase *in situ via* a confinement induced isotropic to lamellar phase transition. This avoided problems resulting from the viscosity and turbidity normally characteristic of these lamellar phase samples. Increasing the amount of PEG resulted in a marked decrease in the layer compressibility modulus $\bar{B}$ indicating a decrease in the repulsive forces between the lamellae. The origin of such a phenomenon is discussed in terms of different mechanisms including depletion interactions, bridging interactions and modification of the electrostatic interaction between the lamellae by the polymer.

PACS. 82.70.-y Disperse systems – 64.70.Md Transitions in liquid crystals – 61.25.Hq Macromolecular and polymer solutions; polymer melts; swelling

1 Introduction

Macromolecules such as polymers or proteins may alter significantly the properties of self- assembled structures of amphiphilic molecules in solution [1–6]. Examples include the enhanced stability of red blood cell membranes by their cytoskeleton, the adhesion of vesicles induced by polymers and the rigidification of droplet interfaces in emulsions by proteins [3–6]. Many industrial processes take advantage of these modified properties in the presence of macromolecules, *e.g.* to get colloidal stabilisation, to favour a particular state of surfactant organisation (*e.g.* fabric conditioners), to enhance the purification of proteins (by phase separation) or to affect the rheological response (lubricants) [1,2]. From the fundamental research point of view, most of the surfactant-polymer investigations have focused on dilute systems of surfactant [1]. In particular the conformation of polymeric chains in an isotropic environment of mixed micellar solutions is now firmly established. However, in recent years an interest has been increasingly directed towards the study of polymers effects on more concentrate surfactant solutions, especially on the lamellar phases (L_α phase) [7–20]. The lamellar phases are Liquid-Crystal Smectic A phases which consist in planar stacks of bilayers, containing surfactant and cosurfactant molecules, separated by a solvent. The properties of these phases are now fairly well-known [21]. Such surfactant lamellar phase-polymer systems are very interesting to study since a diverse set of physical situations can be realised. Different properties and behaviours can be achieved by playing with the inter-membrane interactions and the surfactants (and/or solvent)/polymer interactions. Depending on the polymer interactions with the surfactants (and/or the solvent), the polymer can be localised entirely in the membrane [9,20], both in the membrane and in the solvent [8], adsorbed onto the bilayer surface [13,16,17], or localised entirely in the solvent [11,12,19]. Therefore, the addition of a polymer to a lamellar phase can influence the inter-membrane interactions by altering the structure of the bilayers (*i.e.* the bilayer thickness and the area per surfactant head group) and the elastic constants of the membranes. Moreover, the polymer can induce an additional inter-membrane interaction *via* depletion [11,12] or bridging [17]. The inter-membrane interactions can be tuned by the choice of the surfactant

[a] *Present address*: Laboratoire de physique, École Normale Supérieure de Lyon, 69364 Lyon Cedex 07, France.
e-mail: `efreyssi@physique.ens-lyon.fr`
[b] *Present adress*: Équipe Mixte CEA-Rhône Poulenc, Service de Chimie Moléculaire, CEA Saclay, 91191 Gif/Yvette Cedex, France.
[c] *Present address*: Institut Charles Sadron - CNRS, 6 rue Boussingault, 67083 Strasbourg Cedex, France.
[d] *Present address*: Complex Fluids Laboratory - CNRS-Rhône Poulenc, UMR 166, Prospect Plains Road, Cranbury, N.J. 08512, USA.

and solvent. Electrostatic interactions will be favoured for ionic surfactants when the solvent will be low in salt, but undulation interactions will be dominant for non-ionic surfactants or systems containing high levels of salt or if an oil is used as the swelling agent. Thus, the study of such systems has recently developed both theoretically [12,22–24] and experimentally [7–20] with most of the studies concentrating on systems composed of water-soluble uncharged polymers and ionic surfactants.

In this article we present an experimental study on such a system which aims to characterise the effect of polymer addition on the inter-membrane interactions, and hence the overall influence of the polymer on the phase behaviour. The origin of the present study comes from the work done by Ficheux *et al.* [13,14] on lamellar phases made up of: sodium dodecyl sulfate (SDS), octanol, water-polyethylene glycol (PEG) mixture. One important observation made by Ficheux and co-workers [13,14] was that an increase in the PEG concentration destabilised the lamellar phase. The overall mechanism for this is thought to be a softening of the repulsive interactions between the bilayers which stabilises the lamellar phase due to the presence of PEG. Furthermore, they observed that the decrease in the bilayer-bilayer repulsive interactions was more pronounced as the size of the PEG macromolecule approached the characteristic distance between two neighbouring membranes.

Nevertheless, the way PEG decreases the inter-bilayers repulsive interaction is not understood yet. In absence of PEG in water, such lamellar phases (from SDS/alcohol/water systems) are simply stabilised by electrostatic repulsive interaction whose the interaction potential per unit area $V(d)$ is given by:

$$V(d) = \frac{k_{\mathrm{B}}T}{4L_{\mathrm{B}}(d-\delta)}\left[1 - \frac{\Sigma}{L_{\mathrm{B}}(d-\delta)} + \left(\frac{\Sigma}{L_{\mathrm{B}}(d-\delta)}\right)^2\right] \quad (1)$$

where d is the lamellar period, δ is the bilayer thickness, $L_{\mathrm{B}} = \pi e^2/\varepsilon k_{\mathrm{B}}T$ is the Bjerrum length of the solvent and Σ is the area per charge. Thus, addition of PEG could induce an attractive contribution that would come to superimpose to the natural electrostatic repulsion given by equation (1) (such depletion or bridging). Or, on the other hand, the addition of PEG could modify the classical electrostatic interaction which, then, would be no longer described by equation (1).

To understand the mechanism leading to this decrease in the repulsion more quantitative information about PEG concentration effects on the interactions between the SDS/alcohol bilayers in the L_α phase are required. Such information may be obtained experimentally by measurements of the compressibility modulus $\bar{B}$ as function of the polymer concentration. The compressibility modulus is directly related to the interactions between the membranes [21,25] and therefore gives useful insights into stability of lamellar phase. The value of $\bar{B}$ can be measured using various techniques [21], but most of them lead to a combination of $\bar{B}$ with the other smectic elastic constants K [21]. Direct measurements of $\bar{B}$ are possible *via* three techniques namely: the study of the baroclinic mode relaxation using dynamic light scattering [25,26], the response of a stack of layered membranes confined between two rigid surfaces using a Surface Force Apparatus (SFA) [27–30], and the osmotic stress technique [31,32]. The baroclinic mode relaxation technique requires very well oriented samples which are difficult to obtain with the SDS/Octanol/water-PEG system and so Ficheux *et al.* were not able to measure the evolution of $\bar{B}$ as a function of the PEG concentration in their light scattering study [13,14]. Therefore, the aim of this work was to measure the value of $\bar{B}$ as a function of the PEG concentration using the Surface Force Apparatus technique.

The compressibility modulus of a lamellar phase can be measured using the SFA since these layered systems have a well defined elastic response when confined between two rigid surfaces. The technique has been extensively described in literature for a number of different lamellar phases [27–30]. In brief, the elastic response of a layered system, when properly aligned between the two surfaces of the SFA, gives rise to a force-distance profile with parabolic oscillations. The parabolic shape originates from the elastic response of the confined stack of lamellae. In a simple view, the stack of lamellae can be seen as a series of identical springs joined lengthwise. The springs each have the same spring constant and so the deformation is uniform across all of the springs. Therefore, the shape of the parabolic branches depends on the value of the compressibility modulus $\bar{B}$ of the lamellar phase. The oscillations themselves arise as edge dislocations are induced (or annihilated) to retain the lowest energy configuration whenever surface separation, D, is not commensurate with the equilibrium periodicity of the lamellar phase [29]. It has been shown that, neglecting the energy associated with the dislocations themselves, the elastic free energy of a confined membrane stack can be related to the measured force $F(D)$ as follows [29]:

$$\frac{d_n(F(D)) - F(d_n))}{\pi R} = \bar{B}(D - d_n)^2 \quad (2)$$

where d_n is the position of the oscillation minimum and R the surfaces mean radius of curvature. The force-distance profile, therefore, allows the measurement of the layer compressibility modulus of the lamellar phase from the shape of the oscillations [27–30]. The experimental data from each oscillation plotted as; $d_n(F(D) - F(d_n))/\pi R$ *versus* $(D - d_n)^2$, lie on a straight line the slope of which representing the compressibility modulus, $\bar{B}$.

Unfortunately, due to some technical reasons explained further below, the lamellar phases of SDS/alcohol/water-PEG mixture systems could not directly be measured with the SFA used for this study. The problem has been overcome by working with a bulk micellar phase (L_1 phase) close to the micellar to lamellar phase transition. Confinement of such a fluid between two smooth rigid walls results in a phase transition to a lamellar phase that is stable as long as the confining field is maintained. In this way, the elastic properties of the induced lamellar phase could indeed be measured and the influence of the incorporation

of a polymer into the system could be evaluated. Since the procedure relies on the confinement induced micellar to lamellar phase transition, some tuning of the system was required in order to reach this transition at a reasonable temperature. This was simply achieved by swapping the octanol cosurfactant for pentanol. Such a replacement deviates slightly from the system studied by Ficheux *et al.* but still provides some useful insight into the mechanism by which the PEG macromolecule can destabilise the lamellar phase. Here, the study has been narrowed to lamellar phases with an interlamellar spacing of the order of the size of the PEG macromolecule.

The interest of working with such systems (SDS/alcohol/water-PEG mixture) is that SDS/PEG interactions are already well-known. Several previous studies have shown that PEG and SDS interact strongly [7,33,34]. In aqueous micellar solutions of SDS, the polymer chains wind around the SDS micelles forming a necklace-type structure [33,34]. In this picture, some PEG segments adsorb at the interface between the water and the hydrophobic tails of the SDS without penetrating into the aliphatic core of the micelle, most of the PEG segments exist in the water phase. A similar polymer/surfactant conformation has also been seen in the case of mixed micelles of SDS and a co-surfactant [35]. Following these results Ficheux *et al.* [13,14] describe their system as a stack of SDS/octanol bilayers carrying adsorbed PEG macromolecules on the bilayer surface. Their experimental data seem to confirm this picture. Once again only a few segments of each PEG chain adsorb at the interface between water and the hydrophobic part of the bilayer, and most of the polymer chain forms a mushroom-like structure or a brush (depending on the concentration) extending into the water layer.

2 Experimental

2.1 Sample preparation

The experimental solutions were prepared by first dissolving dry PEG in Milli-Q water to obtain the required composition. This mixture was then heated and held at 50 °C for two hours, allowed to cool to room temperature, and filtered through a 0.2 μm filter to remove any insoluble material. The water-PEG mixtures formed clear homogeneous solutions at all temperatures and for all compositions investigated. The SFA samples were then simply prepared by weighing SDS, pentanol, and the water-PEG mixture into a flask and stirring thoroughly. The different samples studied always had the following composition; 7.15% (by weight) SDS, 17.35% pentanol, and 75.5% water-PEG mixture. Only the polymer concentration in water was varied from 0 to 20 g/l. The SDS (BDH-special pure) and the polymer (Fluka) were used as received. The pentanol (Sigma-AR) was double-distilled before use. The molecular weight (M_w) and the polydispersity index (M_w/M_n) of the PEG were measured by Ficheux using gel permeation chromatography and found to be 22 600 g/mol and 1.1 respectively [13,14]. The radius of gyration of isolated PEG macromolecules in water, R_g, was 29 Å and the overlap concentration c^* was 35 g/l deduced from neutron and light scattering experiments by Ficheux *et al.* [13,14].

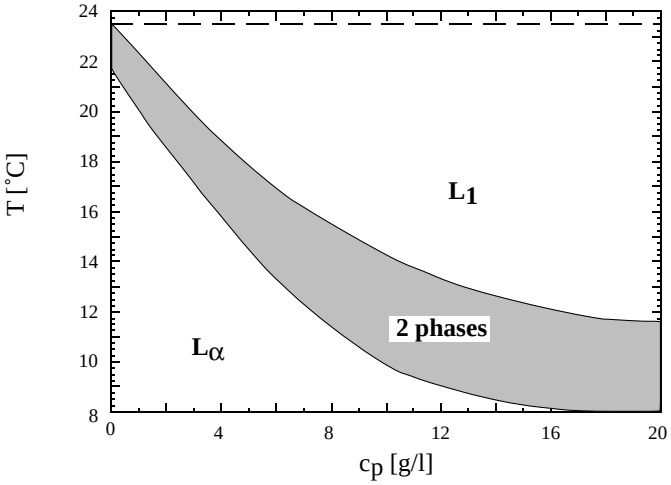

Fig. 1. Phase behaviour of the SDS/pentanol/water/polyethylene glycol (PEG) system containing (by weight) 7.15% SDS, 17.35% pentanol, and 75.5% PEG/water mixture as function of temperature and PEG concentration in water (c_p). L_α is the lamellar phase and L_1 is the micellar phase and 2 phases means the solutions appear as 2 separate phases: L_α and L_1. The SFA experiments were all performed at $T = 23.5$ °C (dashed line); $c_p = 2$ g/l, $\Delta T = 2$ °C; $c_p = 6$ g/l, $\Delta T = 6.5$ °C; $c_p = 12$ g/l, $\Delta T = 10$ °C; $c_p = 18$ g/l, $\Delta T = 12$ °C.

2.2 Phase equilibria

A phase behaviour of the experimental system described above was determined by observations in bulk and by cross polarising microscopy for a series of samples differing in PEG concentration and temperature. This phase behaviour is shown in Figure 1. All experiments were performed at the same temperature of 23.5 °C, which maintained the solutions in the micellar phase over all the polymer compositions studied. We define $\Delta T = T_{exp} - T^*(c_p)$, where T_{exp} is the temperature at which the experiments were performed ($T_{exp} = 23.5$ °C) and $T^*(c_p)$ is the micellar to lamellar bulk phase transition temperature at a given PEG concentration. Over the different values of c_p studied, ΔT varied between 2 and 12 °C.

2.3 X-ray scattering

The smectic periodicity of three solutions of the experimental system in their lamellar state was measured by mean of small angle X-ray scattering (SAXS). The PEG concentrations in water for these solutions (c_p) were: $c_p = 0$, 5, and 10 g/l respectively. The X-ray spectrometer (located in Centre de Recherche Paul Pascal, CNRS, Pessac) used $CuK_{\alpha 1}$ radiation ($\lambda_0 = 1.54$ Å) that was

selected with a germanium monocrystal monochromator from a copper rotating anode source. The resolution of the experiment was set by a series of slits in front of the detector giving a good in-plane resolution function with a half width at half maximum of the order of 10^{-2} Å^{-1}.

2.4 Force measurements

The force-distance profiles were measured between two macroscopic surfaces immersed in the micellar solutions using a Mark IV surface force apparatus (SFA). This technique allows the direct measurement of the interaction force $F(D)$ between two molecularly smooth surfaces as a function of their separation D. The experimental procedure has been well established and documented over the years and is fully described elsewhere [36,37]. The force measurements were carried out on four solutions having the following polymer concentrations in water; c_p = 2, 6, 12, and 18 g/l.

Above it was noted that the lamellar phase of this system could not be directly examined with the SFA. Such lamellar phases are optically turbid and the white light beam that traverses the SFA chamber (through the L_α phase surrounding the surfaces – portion of few mm thick –, the surfaces and the confined fluid between the surfaces) is scattered by the lamellar solution surrounding the surfaces. The interferometric technique (fringes of equal chromatic order, FECO) used to measure the surface separation in the SFA experiments [38] is thereby severely impaired. The micellar phase is however optically clear and, most importantly, transforms into the lamellar phase upon confinement (to be shown below). This confinement induced phase transition, in the gap between the surfaces, therefore allows the properties of the lamellar phase to be studied in the SFA since the bulk phase in the SFA chamber is always in the micellar state. The turbidity due to the layer of induced lamellar phase is not significant since it is very thin (< 500 nm) and furthermore, the lamellae align homeotropically with respect to the SFA surfaces over the whole volume of the induced phase.

Compared to more classical SFA experiments, two major technical problems were encountered in this work due to restrictions imposed by the experimental solutions used. The first one was the degradation of the mica/silver interface often encountered when working with aqueous solutions containing certain anions or anionic surfactants [39,40] including SDS in the present case. To overcome this problem, silica surfaces were used instead of mica since the silver/silica interface is less susceptible to degradation. Thin silica sheets were prepared following the method of Horn *et al.* [41,42] using high purity, synthetic silica (Suprasil, Heraeus). The second problem was the dissolution of the resin (Epikot 1004, Shell) used to stick the surfaces onto the cylindrical lenses of the SFA due to the solvent properties of the samples. Dissolution of the glue was prevented by adding a cross linking agent to the Epikot resin to render it insoluble. The resin used for this work was prepared by mixing Epikot 1004 and the cross-linking agent (EPF108, Shell) in acetone and di-methyl sulfoxide in the ratio 47:6:30:7 by weight. A thin layer of this mixture was spread onto the lenses after which all the solvent was removed *in vacuo* (at 2×10^{-3} Torr for 30 hours). The lenses were then heated to approximately 100 °C to melt the resin at which time the thin silica sheets were glued, silver side down, onto the lenses. The temperature was increased to ≈ 160 °C for 1 h to allow the resin to completely polymerise. Immediately prior to installation into the SFA, the silica surfaces were treated with a water plasma (125 kHz, at 10 W for 30 s, P_{H_2O} = 0.065 Torr, P_{Ar} = 0.02 Torr) to remove any organic contaminants.

The procedure developed by Horn and Smith for the asymmetric interferometer [42] was used to calculate the surface separation. By using silica surfaces and a cross linked resin, the SFA experiments could be carried out over several days (typically one week) allowing time to check the reproducibility of the force runs.

3 Results

Displayed in Figure 1 is the phase behaviour of these particular solutions (with the composition; 7.15% SDS, 17.35% pentanol, and 75.5% water-PEG mixture), both as function of the polymer concentration in water, c_p, and temperature, T. The first qualitative observation is that an increase in the polymer concentration in water favours the micellar phase rather than the lamellar phase. That is, the temperature of the micellar (L_1) to lamellar (L_α) transition is pulled down as the PEG concentration increases ($T^* \approx$ 23.5 °C and 12.5 °C at 0 g/l and 20 g/l of PEG respectively). Above 20 g/l of PEG in water, whatever the temperature, the lamellar phase could never be observed. Bellow T^* (*i.e.* for $T <$ 12 °C), the solutions always appeared as two separate phases; L_1 and L_α.

Figure 2 shows the X-ray scattering curves obtained for the three different solutions in their lamellar state. The X-ray spectrometer resolution was good enough to allow an accurate measurement of the lamellar period of these solutions ($\Delta d \approx$ 1 Å) and see any significant polymer effect on the lamellar structure. The smectic periodicity d of the lamellar structure was extracted from the position of the first-order Bragg diffraction peak q_0 using; $d = 2\pi/q_0$. Furthermore, the SDS/pentanol bilayer thickness could be estimated for each PEG concentration since $\delta = d/(1 - \phi_{sol})$. The parameter ϕ_{sol} is the solvent volume fraction taking into account the small amount of pentanol dissolved in the water-PEG component. We assume that this amount was equal to the amount of pentanol soluble in pure water and so, $\phi_{sol} \approx$ 76% [43]. The measured values of d and estimated values of δ, displayed in Table 1, show that an increase in PEG concentration in water does not have any significant effect on neither the lamellar structure nor the bilayer thickness. This result is in agreement with the results obtained by Ficheux and co-workers on the SDS/octanol/water-PEG system [13, 14]. The estimated values for δ are also in agreement with the values previously reported in the literature for such

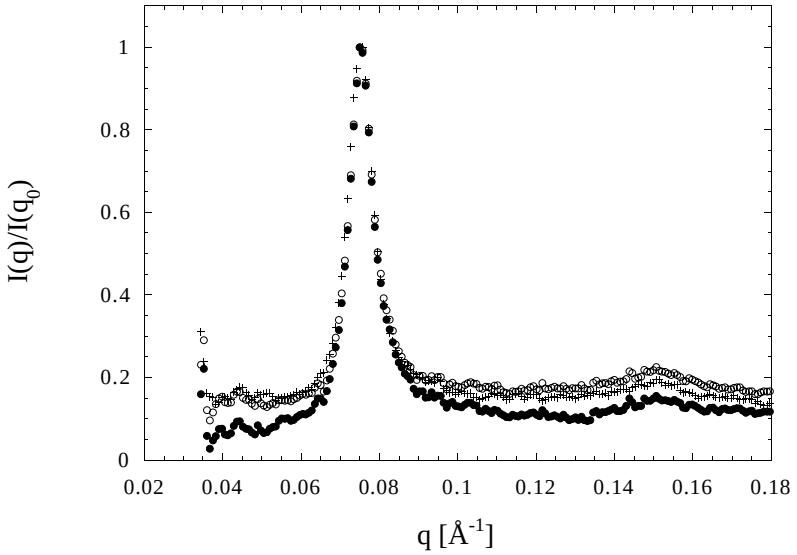

Fig. 2. Small angles X-ray scattering curves ($I(q)/I(q_0)$ *vs.* the wave vector q) obtained for samples with the following composition (by weight); 7.15% SDS, 17.35% pentanol and 75.5% water-PEG mixture, in their lamellar state. The PEG concentration in water were; 0 (•), 5 (○) and 10 (+) g/l respectively.

Table 1. Periodicity of the lamellar phase d and bilayer thickness δ of; 7.15% SDS, 17.35% pentanol and 75.5% water-PEG mixture solutions in their lamellar state for the different PEG concentrations studied. These values are deduced from the scattering curves displayed in Figure 2. d is extracted from the position of the first-order Bragg diffraction peak q_0 using $d = 2\pi/q_0$ while the bilayer thickness is estimated using $\delta = d/(1-\phi_{\rm sol})$. $\phi_{\rm sol}$ is the solvent volume fraction taking into account the small amount of pentanol soluble in the water-PEG mixture, that is $\phi_{\rm sol} \approx 76\%$.

$c_{\rm p}$ [g/l]	d [nm]	δ [nm]
0	8.4 ± 0.1	2.02 ± 0.05
5	8.4 ± 0.1	2.02 ± 0.05
10	8.3 ± 0.1	1.99 ± 0.05

bilayers [44]. However, the resolution of the SAXS camera was unfortunately, not good enough to allow a shape analysis of the scattering curves (*i.e.* scattering at very small angles and scattering around the Bragg diffraction position). Therefore, no qualitative information about a PEG effect on the interactions between SDS/pentanol bilayers in lamellar phase could be deduced from these data in the same way as Ficheux *et al.* [13,14].

Figure 3 shows the force-distance profiles upon approach and separation of the two surfaces confining each of the four samples studied. The force-distance profiles exhibit similar features whatever the PEG concentration.

On approach of the surfaces (filled circles) an attractive background force is seen over which regular oscillations are superimposed until a strong repulsive barrier is reached. The range and the magnitude of the attractive background decreases as the polymer concentration in water increases. The position of the steep repulsion near contact remains independent of the polymer concentration and was always found at a surface separation of about 9.0 nm with respect to the bare silica-silica contact measured in dry nitrogen. The magnitude of the oscillations increases as the separation between the walls decreases. The magnitude and hence the number of oscillations measurable within the sensitivity of the technique ($\Delta F = \pm 10^{-2}$ mN/m) decreases as the polymer concentration in water increases. Note that the surfaces remain at stable separations only in regions where the slope of the force $\partial F/\partial D$ is less than or equal to the SFA spring constant k. When this slope is larger than the spring constant the surfaces are seen to jump from one stable position to another. The inward "jump" from one stable position to the next occurred quite quickly (typically 1 s) for the solution with 2 g/l of PEG and somewhat slower (of the order of 10 s) for the solution with 18 g/l of PEG.

Upon separation of the surfaces (open circles) after reaching the steep repulsion near contact, an adhesive minimum was seen from which the surfaces jumped apart and came to rest at some large separation, where no oscillation can be observed. Whatever the polymer concentration, several minutes were required to allow the surfaces to stabilise at this new position. For surface separation larger than this distance, the forces measured upon further separation showed similar behaviours as the forces measured during the inward force runs.

Although the oscillations appear to occur at regular intervals during the approach of the surfaces, the best measure of the periodicity of the oscillatory profile is obtained from the distance between adjacent force minima. Due to the above mentioned spring instability, the force minima of the oscillations generally need to be measured upon separation of the surfaces [27–30]. However, pulling the surfaces out of the adhesive minima located at around 9.0 nm causes a jump to large surface separation, missing the oscillations seen during the approach of the surfaces.

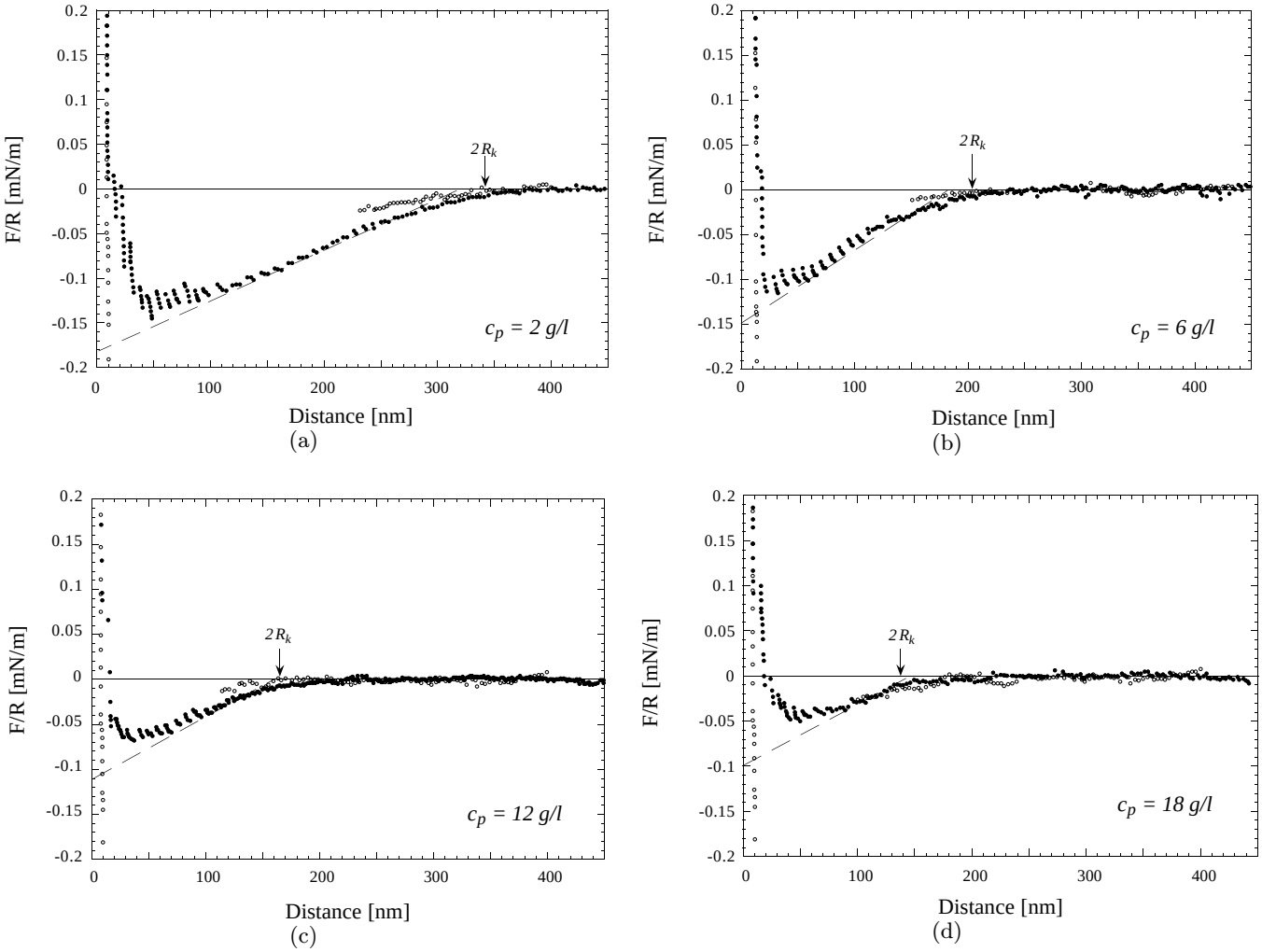

Fig. 3. Forces F (normalised by the surfaces mean radius of curvature, R) as a function of the separation between two silica surfaces immersed in SDS/pentanol/water and PEG micellar phases. Measurements recorded at $T = 23.5$ °C: (a) $c_\mathrm{p} = 2$ g/l, (b) $c_\mathrm{p} = 6$ g/l, (c) $c_\mathrm{p} = 12$ g/l, (d) $c_\mathrm{p} = 18$ g/l. The filled circles (•) correspond to the force-distance profiles measured upon reducing the surface separation. The open circles (○) correspond to the force-distance profiles measured upon separation of the surfaces. The dashed straight lines in Figure 3 define the attractive background used to estimate the $\mathrm{L}_\alpha/\mathrm{L}_1$ interfacial tension.

Hence, specific measurements were carried out at each composition to recover the information lost in this unstable regime by performing several approach/separation cycles. Each oscillation was first located during the approach of the surfaces. Once located, the surfaces were moved apart to measure the force profile of the oscillation down to the force minimum. This was repeated for as many oscillations as possible without pushing the surfaces all the way down to contact, thus avoiding interference from the primary adhesive minimum. Even so, as the magnitudes of the oscillations are weak and decrease quickly with their rank, due to the sensitivity limit of the technique ($\Delta F = \pm 10^{-2}$ mN/m), only some of the oscillations seen upon compression were able to be accurately measured upon separation to allow a shape analysis. Typically up to six oscillations could be measured as shown in Figure 4. For each measured oscillation, both the shape and the force magnitude obtained during different cycles were always very similar (except for the one closest to zero separation). In Figure 4 the oscillations are plotted as $(F(D) - F(d_n))/R$ as a function of D, where $F(d_n)$ is the non-zero force at the minimum of the oscillation, since the absolute force with respect to the original baseline is lost during the forwards and backwards cycling. As a consequence the envelope that delimits the minima of the force oscillations, and hence the overall magnitude of the attractive background, was not known precisely.

4 Analysis and discussion

For such isotropic solutions of micelles, one would expect the force-distance profiles to be constant and around zero,

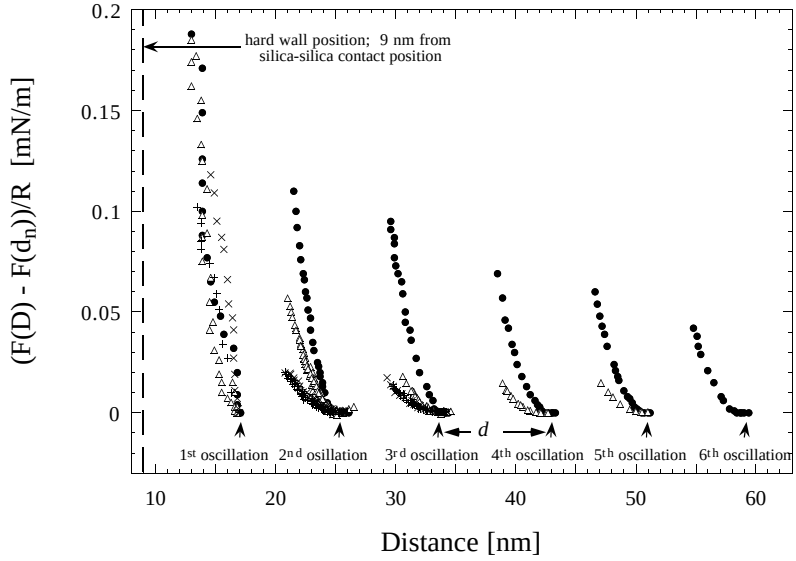

Fig. 4. Force-distance profile of each oscillation measured upon separation of the surfaces for each sample studied; $c_p = 2$ g/l (•), $c_p = 6$ g/l (△), $c_p = 12$ g/l (×), $c_p = 18$ g/l (+). In each case the overall background force has been set to zero by plotting $(F(D) - F(d_n))/R$, where $F(d_n)$ is the non-zero force of the oscillation minimum, since the absolute force with respect to the original baseline is lost during the forwards and backwards cycling. Whatever the PEG concentration the oscillation periodicity is; $d = 8.4 \pm 0.3$ nm.

with a depletion attraction between the surfaces occurring at about 20-30 nm from the silica-silica contact position [45]. Thus the onset of an attraction between the surfaces at separations larger than 100 nm is an indication that the confined micellar film has undergone a transformation. The oscillatory behaviour superimposed on the attractive background gives information about this transformation. Indeed, this oscillatory behaviour indicates the presence of strong correlations inside the confined liquid film. By comparing the distance between adjacent minima it can be seen that the oscillations are periodic (Fig. 4). Whatever the PEG concentration in water, the periodicity was equal to 8.4 ± 0.3 nm which is in excellent agreement with the measured smectic periods by means of SAXS experiments (see Tab. 1). This is the first indication that the bulk micellar solutions undergo a phase transformation to an induced lamellar structure upon confinement. This claim is further supported by observing that all the oscillations have a parabolic shape (Figs. 4, 5 and 6) arising from the elastic response of a confined lamellar phase upon compression or decompression [27–30]. (It should be notted that in the present work, even with values of ΔT equal to 12 °C, the L_1/L_α transformation could always be reached by means of confinement.)

Similar confinement induced ordering transitions have previously been observed for several other isotropic surfactant phases including the sponge phase and microemulsion phases [40,46–49]. Milner *et al.* have studied isotropic to lamellar phase transitions of this kind theoretically [50]. In the present case, the transition of the micellar phase to the lamellar structure can be seen as a surface induced ordering of an isotropic fluid to a layered structure that is more compatible with the topology of flat rigid surfaces. When the surfaces have large curvature radii capillary condensation phenomenon is monitored by the balance between an unfavorable volume contribution and a favorable interfacial contribution.

Note that in the present system, the measured periodicity of the oscillations indicates that the characteristic defect observed in the induced lamellar phase was an edge dislocation of Burgers vector $b = 1$. That is, each of the force discontinuities in Figure 3 corresponds to an edge dislocation being created in the center of the confined film and the number of layers being reduced from n to $n - 1$.

4.1 The attractive background

As soon as the lamellar phase has condensed, an attraction between the surfaces arises because the lamellar structure is induced only in a central droplet in the gap and remains surrounded by bulk liquid which is still in the micellar state. Such a behaviour has already been observed when a lamellar phase was induced by confinement of a sponge phase [40,46,47] or a bicontinuous microemulsion phase [48,49] and is a general feature of capillary condensation phenomena [51–54].

To begin a more quantitative analysis of the background attraction we assume that before the micellar to lamellar transformation a thin lamellar film wets each silica surface. The lamellar film thickness on each surface is h and the L_α/L_1 interface area is $2A$, where A is the silica surface area. This interface has an associate surface tension $\gamma_{||}$ (*i.e.* the smectic layers are parallel to the lamellar-micellar interface). After the transition, the induced droplet of L_α phase has a volume V, covers the former L_α/L_1 interface over a surface area A_1

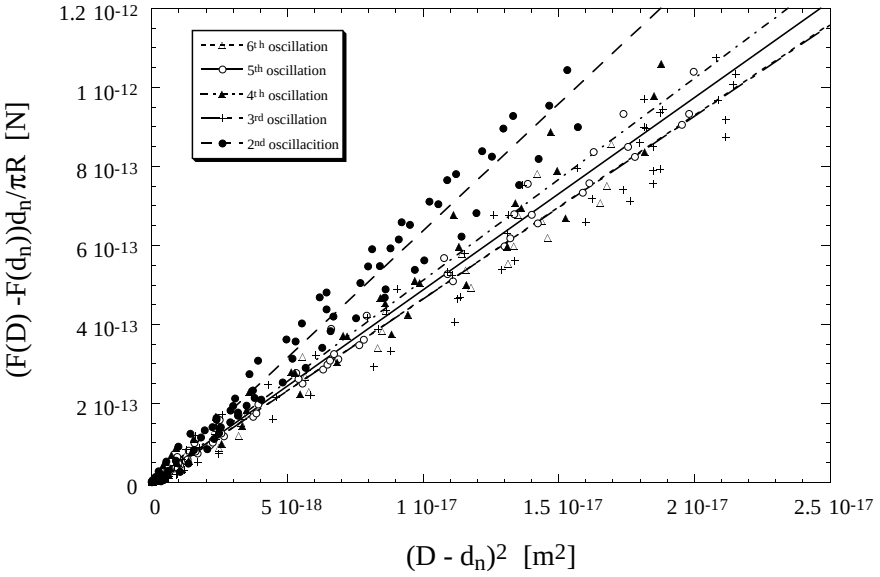

Fig. 5. Plot of each oscillation observed in Figure 4 for the sample with $c_{\rm p} = 2$ g/l as: $(F(D) - F(d_n))d_n/\pi R$ *versus* $(D-d_n)^2$. The slope of the curves represents $\bar{B}$ as shown by equation (2) where $F(D)/2\pi R$ is the elastic energy density of the nth parabola centred at d_n (n smectic layers at zero stress confined in the gap). The data give: (•) $\bar{B}_{\rm 2nd} = 65400 \pm 3500$ Pa, (+) $\bar{B}_{\rm 3rd} = 48400 \pm 3000$ Pa, (▲) $\bar{B}_{\rm 4th} = 52200 \pm 3000$ Pa, (○) $\bar{B}_{\rm 5th} = 49700 \pm 3000$ Pa, (△) $\bar{B}_{\rm 6th} = 48500 \pm 3000$ Pa, for the 2nd, 3rd, 4th, 5th, and 6th oscillation from contact respectively. The value of $\bar{B}$ for this sample is taken as the average of all the slopes ($\bar{B}_{n\rm th}$) and the uncertainty is the largest deviation from the mean value. Thus, here $\bar{B}$ is equal to $(5.3 \pm 1.2) \times 10^4$ Pa.

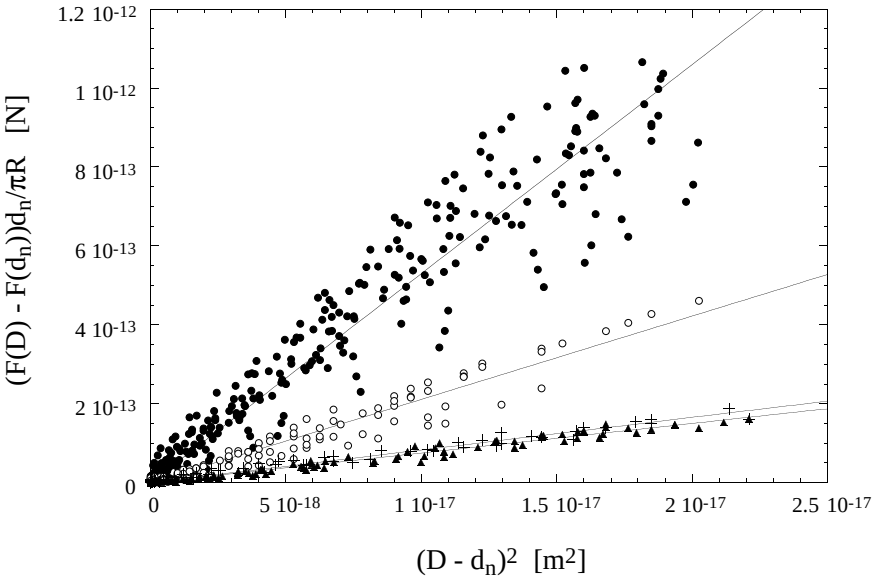

Fig. 6. Plot of $d_n(F(D)-F(d_n))/\pi R$ *versus* $(D-d_n)^2$ for each of the samples studied; $c_{\rm p} = 2$ g/l (•), $c_{\rm p} = 6$ g/l (○), $c_{\rm p} = 12$ g/l (+), $c_{\rm p} = 18$ g/l (▲). The slope of each straight line corresponds to the mean value of $\bar{B}$ obtained for the considered sample as explained in the text (and in Fig. 5 caption). These values are also summarised in Table 3.

and creates an additional L_α/L_1 interface surrounding the condensed droplet. This new L_α/L_1 interface of surface area A_2 has an associate surface tension $\gamma_\perp$ (*i.e.* the smectic layers are perpendicular to the lamellar-micellar interface). Following the results obtained by Quillet *et al.* for the lamellar-sponge interfacial tension [55], in what follows we will assume; $\gamma_\parallel \gg \gamma_\perp$. The free energy variation associated with the capillary condensation of the lamellar phase, ΔG, will therefore contain three competing contributions. i) The free energy gain of the confined system by annihilating some of the interface between the thin lamellar film prewetting each silica surface and the "bulk" micellar phase. This lost of L_α/L_1 interface gives: $\Delta G_1 = -\gamma_\parallel A_1$. ii) The free energy increase due to the new created L_α/L_1 interface, that is: $\Delta G_2 = \gamma_\perp A_2$. iii) Finally, transforming a droplet of the equilibrium bulk micellar phase to the metastable confined phase represents an increase in the free energy: $\Delta G_3 = \mu V$, where μ is the difference

in density of free energy between the two phases. Thus the total change in free energy upon capillary condensation of a L_α phase is: $\Delta G = -\gamma_\parallel A_1 + \gamma_\perp A_2 + \mu V$. (It is clear that ΔG_1 provides the only favourable contribution to the total free energy of forming a capillary condensate of lamellar phase and therefore describes the driving force for the micellar to lamellar transition.) Since the surfaces have large curvature radii, the parameters V, A_1 and A_2 can be related to the surface separation D as follows: $V \approx \pi R_m^2 \left((D-2h) + R_m^2/4R\right)$, $A_1 \approx \pi R_m^2 (2 + R_m^2/4R^2)$ and $A_2 \approx 2\pi R_m \left((D-2h) + R_m^2/2R\right)$ [48,54,56]. R is the surfaces mean radius of curvature and R_m is the radius of the induced L_α phase droplet that is given by minimising the free energy ΔG with respect to R_m. The typical operational distances in such SFA experiments are: $R \approx 10^{-2}$ m, $R_m \approx 10^{-5}$ m, $D \approx 0{-}10^{-6}$ m and $2h \approx 10^{-9}{-}10^{-8}$ m. Thus, since $R \gg R_m \gg D - 2h$ and $\gamma_\parallel \gg \gamma_\perp$, the ΔG_2 contribution to the total free energy variation can be neglected and the minimisation of ΔG with respect to R_m gives $R_m \approx \sqrt{2R[2R_k - (D-2h)]}$, where $R_k = \gamma_\parallel/\mu$ is the Kelvin radius. $2R_k$ gives the largest surface separation at which the capillary condensation can occur. Thus, when $D - 2h > 2R_k$, the induced droplet cannot exist between the surfaces and $F(D) = 0$ [48,54,56]. When $D - 2h < 2R_k$, in first approximation, the resulting interaction between two crossed cylinders having large curvature radii can be written as;

$$\frac{F(D)}{R} = -\frac{1}{R}\left(\frac{\mathrm{d}\Delta G}{\mathrm{d}D}\right) = -\frac{1}{R}\left(\frac{\partial \Delta G}{\partial D}\right) \approx -4\pi\gamma_\parallel \left(1 - \frac{D-2h}{2R_\mathrm{k}}\right). \quad (3a)$$

Experimentally $2R_\mathrm{k}$ is found of the order of 10^{-7} m (Fig. 3), thus $h/R_\mathrm{k} \ll 1$. Hence, equation (3a) becomes:

$$\frac{F(D)}{R} \approx -4\pi\gamma_\parallel \left(1 - \frac{D}{2R_\mathrm{k}}\right). \quad (3b)$$

Clearly, the force-distance profile is attractive and linear the slope of which being proportional to the free energy density difference between the "bulk" phase and the condensed phase while the intercept is related to the interfacial tension between these two phases. It should be noted that if the L_α/L_1 surface tension anisotropy is ignored, then, it is found the force already derived by different authors for capillary condensation phenomena in different systems [48,54,56].

Since in the present study the induced phase is a lamellar phase, a second contribution, that takes into account the classical elastic response of a lamellar phase under confinement [29] must be added to the total free energy. Thus, the overall storing force between the macroscopic crossed-cylinder surfaces is given by [49,57]:

$$\frac{F(D)}{R} \approx -4\pi\gamma_\parallel \left(1 - \frac{D}{2R_\mathrm{k}}\right) + \pi\bar{B}\frac{(D-d_n)^2}{d_n}. \quad (4)$$

Equation (4) indicates that the force-distance profile for a confined droplet of lamellar phase surrounded by a bulk phase will be a set of regularly spaced parabolic oscillations whose minima fall on a linear attractive background. Such force-distance profiles were indeed observed in references [40,46–49,57]. An important property of equation (4) is that it allows the interfacial tension of the interface separating the two phases, γ, and the difference of free energy density between the "bulk" and the condensed phases, μ to be measured. In practice a line of best fit is defined for the data and μ is given by the slope while γ is given by the intercept at $D = 0$ where $F(D)/R = -4\pi\gamma_\parallel$. In this way, the interfacial tension and the free energy density difference between bicontinuous microemulsion phases and lamellar phases have been measured in the case of sodium bis(2-ethylhexyl) sulfosuccinate (AOT)/decane/brine system [48] and tetra-ethyleneglycol mono-n-decylether ($C_{10}E_4$)/octane/water system [49]. The interfacial tension and the free energy density difference between the lamellar phase and the sponge phase has also been measured experimentally in the system AOT/brine [57].

In the present study, only an estimate of $\gamma_\parallel$, μ and $2R_\mathrm{k}$ can be obtained since the position of the oscillation minima were not measured on an absolute scale (see Fig. 4). Nevertheless, the minima seen in the force-distance profiles presented in Figure 3 measured upon approach of the surfaces fall on a reasonably linear envelope (it must be kept in mind that these will not be the true minima of each parabola). The onset of the attraction gives an estimate of $2R_\mathrm{k}$ while the dashed lines in Figure 3 give an estimation of the background attraction from which $\gamma_\parallel$ and μ can be obtained. The resulting values of $\gamma_\parallel$, μ and $2R_\mathrm{k}$ as function of the PEG concentration are summarised in Table 2 and show a decrease of $\gamma_\parallel$ and R_k and a slight increase in μ as the polymer concentration increases. The variations of R_k and μ were expected since ΔT ($\Delta T = T_\mathrm{exp} - T^*(c_\mathrm{p})$) increases with PEG concentration [49,57]. The decrease in the interfacial tension between the L_α and L_1 phases as the PEG concentration increases is, to our knowledge, not predicted by any theoretical model and was never observed before. Nevertheless, we cannot draw any conclusion on the effect of PEG on the interfacial tension between such micellar and lamellar phases since we do not know the effect of ΔT on the L_α/L_1 interfacial tension. Therefore, both more experimental data and theoretical models are required to confirm and understand such a behaviour.

4.2 Measurement of $\bar{B}$ from the experimental data

Once the lamellar phase is condensed between the surfaces it is possible to measure its elastic properties. The layer compressibility modulus of the lamellar phase, $\bar{B}$, is deduced from the shape of the oscillations measured upon separation (except from the 1st oscillation since it corresponds to only one confined bilayer between the surfaces). Some limits are imposed since it was never possible to accurately measure the shape of the oscillations beyond the 6th oscillation due to the sensitivity limits of the technique. With only few bilayers in the confined region there is a danger that the measured oscillations lead to a slightly

Table 2. Estimation of $2R_k$, the interfacial tension, $\gamma_\parallel$, and the difference of free energy density, μ, between the micellar phase and the lamellar phase for the different PEG concentrations studied. Results were extracted from Figure 3. Note the obtained values of $\gamma_\parallel$ are of the same order as those obtained values for the microemulsion or sponge phases and the lamellar phases [48,49,57].

c_p [g/l]	estimation of $2R_k$ [nm]	straight line intercept at $D = 0$; $-4\pi\gamma_\parallel$ [mN/m]	estimation of $\gamma_\parallel$ [mN/m $\times 10^{-3}$]	estimation of μ [J/m^3]
2	340 ± 10	−0.18 ± 0.01	15 ± 0.7	93 ± 9
6	210 ± 10	−0.15 ± 0.01	12 ± 0.7	114 ± 15
12	165 ± 10	−0.11 ± 0.01	9.5 ± 0.7	115 ± 15
18	135 ± 10	−0.095 ± 0.01	8 ± 0.6	118 ± 18

Table 3. Summary of the mean layer compressibility modulus measured for each PEG concentration (see Fig. 6). Since the data set was small the uncertainy in $\bar{B}$, $\Delta\bar{B}$, was taken as the largest deviation from the mean value.

c_p [g/l]	$\bar{B}$ [Pa]	$\Delta\bar{B}$ [Pa]
2	5.3×10^4	$\pm 1.2 \times 10^4$
6	2.1×10^4	$\pm 5 \times 10^3$
12	8.2×10^3	$\pm 2.5 \times 10^3$
18	7.5×10^3	$\pm 2.5 \times 10^3$

overestimated value of $\bar{B}$ due to the influence of the nearby rigid walls. Indeed, it has been shown experimentally that the first few oscillations measured at small separations do not always give the true bulk compressibility modulus [27,28,30,49]. This is particularly important for lamellar systems stabilised by undulation forces [30,49]. The hard walls restrict the bilayer fluctuations and lamellae appear less compressible than the same lamellae in a (thick) bulk lamellar sample. Nevertheless, for systems stabilised by electrostatic forces, as in this case, the values of $\bar{B}$ extracted from the oscillations close to the contact position give a fairly good estimation of $\bar{B}$ [27,28]. (Although the 2nd oscillation from contact always gives a slightly overestimated value of $\bar{B} - \bar{B}_{2\mathrm{nd}}-$ by about 20% since there are only two bilayers confined between the surfaces). To illustrate that, Figure 5 shows the oscillations, measured upon separation, for the sample with 2 g/l of PEG. The oscillations are plotted as $d_n(F(D) - F(d_n))/\pi R$ *versus* $(D - d_n)^2$. In agreement with equation (2) the data lie on straight lines the slopes of which representing the values of $\bar{B}$ for each oscillation ($\bar{B}_{n\mathrm{th}}$). As expected the value of $\bar{B}_{2\mathrm{nd}}$ is slightly higher than the others that are all within the experimental uncertainty (see Fig. 5 caption).

When each measured oscillation has been analysed, the value of the layers compressibility modulus of an investigated lamellar phase is taken as the average of the different $\bar{B}_{n\mathrm{th}}$ and the uncertainty as the largest deviation from the mean value. In Figure 6 the data for all of the samples studied are shown in a plot of $d_n(F(D) - F(d_n))/\pi R$ *versus* $(D - d_n)^2$. The slope of the displayed straight lines corresponds to the obtained mean values of $\bar{B}$ for each sample, which have also been summarised in Table 3. By comparison, Ficheux *et al.* [13], using dynamic light scattering, have investigated the relaxation of the baroclinic mode of a lamellar phase of the SDS, octanol, water and PEG ($M_w = 22\,600$ g/mol) system, with a reticular spacing of 9 nm and a PEG concentration of 50 g/l. From these data they deduced $\bar{B} = 1.9 \times 10^3$ Pa, which is of the same order of magnitude as the value obtained here for the sample with a PEG concentration of 18 g/l.

4.3 Relation between the induced L_α phase and the bulk L_α phase

Having measured the effects of the PEG concentration on $\bar{B}$ in an induced lamellar phase, it is now necessary to decide if these effects are valid for the pure (bulk) lamellar phase. Indeed, two problems arise.

i) First of all, one should question the influence of ΔT ($\Delta T = T_{\mathrm{exp}} - T^*(c_p)$) on the measured values of $\bar{B}$. In the present work ΔT varies from 2 °C (at 2 g/l of PEG) to 11 °C (at 18 g/l of PEG) and it has been observed, in some systems, that the effect of ΔT on the value of $\bar{B}$ could be not negligible [49]. Indeed, Moreau *et al.* [49] have observed that the value of $\bar{B}$ in the induced lamellar phase from a bicontinuous microemulsion of the $C_{10}E_4$/octane/water system, decreased with increasing ΔT. However, at the same time an increase in the lamellar periodicity d of the induced lamellar phase was observed. On the other hand, values of $\bar{B}$ measured for the lamellar phase induced from the sponge phase of the AOT/brine system, did not show any significant dependence on ΔT nor did the measured periodicity [30, 40]. Both the compressibility modulus and the periodicity remained constant with ΔT and were in agreement with the corresponding measurements made in the pure lamellar phases [30,40]. In the classical description of $\bar{B}$ [12,25,58], $\bar{B} = d(\partial^2 V(d)/\partial d^2)_{\mathrm{eq}}$, where $V(d)$ is the interaction potential between the bilayers per unit area. No effect of ΔT is expected to modify the electrostatic interaction between SDS/pentanol bilayers. Thus, as long as ΔT does not have any effect on the lamellar structure $\bar{B}$ should remain constant with ΔT and equal to the layer compressibility modulus of the pure lamellar phase. In the present work the lamellar periods of the induced lamellar phases are always simillar to those of the pure lamellar phases. Therefore, whatever ΔT, we can assume $\bar{B}$ is the same in the induced lamellar phase and in the pure lamellar phase.

ii) The second problem to consider is the PEG concentration in the induced L_α phase. The micellar to lamellar transition implies that the chemical potentials of the induced lamellar phase and the "bulk" micellar phase are equal, but this does not necessarily ensure equality of the PEG concentration in each phase. However, since the measured periods of the induced lamellar phases correspond to those of pure lamellar phases having the same solvent concentration as the micellar phase used for the experiment, solvent concentration in both phases must be similar. Hence, it is most likely that PEG concentration is always similar in the L_1 and induced L_α phase since the chemical potential of water must be equal in both phases. Therefore, in the following discussion we will assume that each obtained value for $\bar{B}$ corresponds to the layer compressibility modulus of the pure lamellar phase with the same PEG concentration as the "bulk" micellar phase presents in the SFA chamber.

4.4 PEG effects on the interactions between SDS/pentanol bilayers

Table 3 shows that the compressibility modulus of the lamellar phase rapidly decreases as the PEG concentration in water increases. This result is indeed in agreement with the observations made by Ficheux *et al.* on the L_α phases of the SDS/octanol/water-PEG mixture system [13,14]. Therefore the presence of PEG in such lamellar phases causes either a significant enhancement of an attractive contribution which superimposes to the *natural* electrostatic repulsion between the bilayers or a decrease in this inter-bilayer interaction.

1) In order to discover the origin of the influence of the PEG on the inter-bilayer interactions, we can first consider the overall interaction potential per unit area between bilayers of a system containing PEG that can be written:

$$V_{\rm eff} = V_{\rm elec}(d, c_{\rm p}) + V_{\rm pol}(d, c_{\rm p}). \tag{5}$$

Here, $V_{\rm elec}(d, c_{\rm p})$ is the classical electrostatic interaction potential per unit area between the bilayers while $V_{\rm pol}(d, c_{\rm p})$ is the interaction potential between the bilayers (per unit area) of the attractive contribution induced by the presence of PEG in the lamellar phase. At this stage the origin of the polymer contribution is not specified. We assume that in presence of PEG the repulsive electrostatic interaction between SDS/pentanol bilayers, $V_{\rm elec}(d, c_{\rm p})$, is still given by equation (1). The parameters d, δ and Σ of equation (1) are assumed to be constants within the range of PEG concentration used as shown by SAXS measurements. However, the dielectric constant of the solution, ε, changes as the polymer concentration increases. (For pure water $\varepsilon = 80$ C^2 m^{-1} J^{-1} and for pure PEG $\varepsilon = 3$ C^2 m^{-1} J^{-1}.) Thus, for PEG concentrations between 0 g/l and 18 g/l in water, the decrease in ε leads to a slight increase in $L_{\rm B}$ and hence to a slight decrease in $V_{\rm elec}(d, c_{\rm p})$. This small PEG effect on $V_{\rm elec}(d, c_{\rm p})$ will be taken into account in the following discussion.

From equation (5), an expression of the layer compressibility modulus at fixed chemical potential of "bilayer components" and polymers can be derived for this *ternary* lamellar system as follows [12,59]:

$$\bar{B}(c_{\rm p}) = \bar{B}^{\rm Lam}(c_{\rm p}) + \bar{B}^{\rm Pol}(c_{\rm p}). \tag{6}$$

$\bar{B}^{\rm Lam}(c_{\rm p})$ describes the contribution of the classical electrostatic repulsive interaction between the bilayers, given by equation (1), to the total compressibility of the lamellar phase. This is the layer compressibility modulus of the *binary* lamellar phase (*i.e.* bilayers/solvent) at constant chemical potential of "bilayer components" [25]:

$$\begin{aligned}\bar{B}^{\rm Lam}(c_{\rm p}) &= d\left(\frac{\partial^2 V_{\rm elec}(d, c_{\rm p})}{\partial d^2}\right)_{\rm eq} \\ &= \frac{\pi k_{\rm B} T d}{2 L_{\rm B}(c_{\rm p}) \bar{d}^3}\left[1 - \frac{3\Sigma}{L_{\rm B}(c_{\rm p})\bar{d}} + \frac{6\Sigma^2}{(L_{\rm B}(c_{\rm p})\bar{d})^2}\right]\end{aligned} \tag{7}$$

where $L_{\rm B}(c_{\rm p})$ takes into account the variation of $L_{\rm B}$ with the PEG concentration and $\bar{d} = d - \delta$. Assuming that ε decreases linearly with the PEG concentration (which seems reasonable at low PEG concentration such as those used in this work), from equation (7), it can be shown that within the range of PEG concentrations studied:

$$\bar{B}^{\rm Lam}(c_{\rm p}) \approx \bar{B}^{\rm Lam}(0)[1 - 0.0009625\ c_{\rm p}]\ \text{Pa}. \tag{8}$$

Here $\bar{B}^{\rm Lam}(0)$ is the value of $\bar{B}$ in the case of the lamellar phase without polymer. Note that in equation (8), $c_{\rm p}$ is the PEG concentration in g/l. The value of $\bar{B}^{\rm Lam}(0)$ for the lamellar phase containing; 7.15% SDS, 17.35% pentanol and 75.5% water, has previously been measured by Richetti and co-workers using similar SFA experiments and found to be equal to 1.7×10^5 Pa [27].

$\bar{B}^{\rm Pol}(c_{\rm p})$ describes the polymer contribution to $\bar{B}(c_{\rm p})$ and hence describes the effect of PEG on the bilayer-bilayer interactions. An expression of $\bar{B}^{\rm Pol}(c_{\rm p})$ can be derived as function of $V_{\rm pol}(d, c_{\rm p})$ as follows [12,59]:

$$\begin{aligned}&\bar{B}^{\rm Pol}(c_{\rm p}) \\ &= d^2\left\{\left(\frac{\partial^2 V_{\rm pol}}{\partial d^2}\right)_{\rm eq} - \frac{\left[\left(\frac{\partial^2 V_{\rm pol}}{\partial d \partial c_{\rm p}}\right)_{\rm eq} - \frac{1}{d}\left(\frac{\partial V_{\rm pol}}{\partial c_{\rm p}}\right)_{\rm eq}\right]^2}{\left(\frac{\partial^2 V_{\rm pol}}{\partial c_{\rm p}^2}\right)_{\rm eq}}\right\}.\end{aligned} \tag{9}$$

The contribution of $\bar{B}^{\rm Pol}(c_{\rm p})$ to the total (measured) compressibility modulus $\bar{B}(c_{\rm p})$ is easy to estimate from the experimental data, simply by subtracting the part due to the electrostatic interaction between the bilayers to the measured compressibility modulus, that is:

$$\bar{B}^{\rm Pol}(c_{\rm p}) = \bar{B}(c_{\rm p}) - \bar{B}^{\rm Lam}(c_{\rm p}). \tag{10}$$

Taking the value of $\bar{B}^{\rm Lam}(c_{\rm p})$ calculated from equation (8) with $\bar{B}^{\rm Lam}(0) = 1.7 \times 10^5$ Pa, the estimated values of

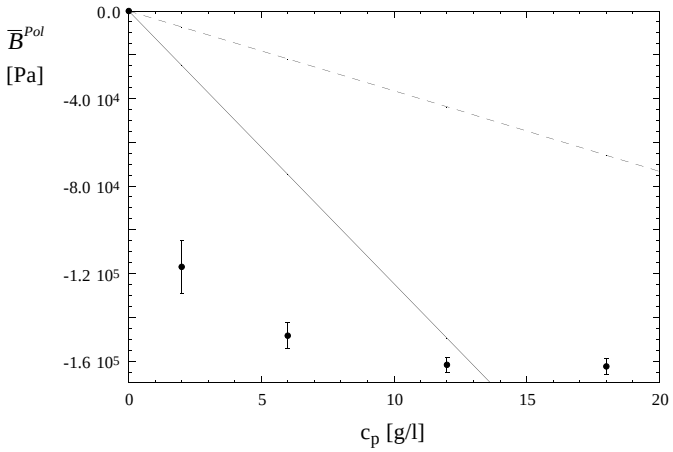

Fig. 7. Polymer contribution $\bar{B}^{\mathrm{Pol}}$ (Eq. (10)) to the total layer compressibility modulus of the lamellar phase $\bar{B}$ as a function of PEG concentration. $\bar{B}$ is the experimentally measured value whereas $\bar{B}^{\mathrm{Lam}}$ is calculated using equation (8) with $\bar{B}^{\mathrm{Lam}}(0) = 1.7 \times 10^5$ Pa. The dashed line corresponds to the behaviour expected for depletion of non-adsorbing polymer according to Ligoure and co-workers [12], when $c_{\mathrm{p}} \ll c^*$ and $\bar{d} = d - \delta \gg R_{\mathrm{g}}$; $\bar{B}^{\mathrm{Pol}} = -4\dfrac{k_{\mathrm{B}}TN^{1/5}d}{a\bar{d}^3}\bar{\phi}$. The plain line corresponds to the behaviour expected in the case of depletion of non-adsorbing polymer with $c_{\mathrm{p}} \ll c^*$ and $\bar{d} = d - \delta \ll R_{\mathrm{g}}$. According to Ligoure *et al.* [12], in that case; $\bar{B}^{\mathrm{Pol}} = -25\dfrac{k_{\mathrm{B}}TNd}{9\bar{d}^4}\left(\dfrac{a}{\bar{d}}\right)^{1/3}\bar{\phi}$. a is the monomer length ($a \approx 5$ Å), N is the polymerisation index ($N \approx 510$), $\bar{\phi}$ is the polymer volume fraction in the solvent (with PEG density taken equal to 1 g/cm^3). Values of parameters a, N and the density are from reference [14].

$\bar{B}^{\mathrm{Pol}}(c_{\mathrm{p}})$ are shown in Figure 7 as a function of PEG concentration in water. At first, the attractive contribution to the interactions between the bilayers is dramatically enhanced as the PEG concentration increases up to a concentration of 6 g/l as evidenced by a drop from $\bar{B}^{\mathrm{Pol}} = 0$ Pa to $\bar{B}^{\mathrm{Pol}} \approx -1.5 \times 10^5$ Pa. Above 6 g/l the strength of this attractive interaction increases much more smoothly ($c_{\mathrm{p}} = 18$ g/l giving rise to $\bar{B}^{\mathrm{Pol}} \approx -1.6 \times 10^5$ Pa). Following this evolution, it can be expected that for PEG concentrations greater than about 20 g/l the attractive part of the bilayer-bilayer interactions will be greater than the repulsive electrostatic interaction stabilising the lamellar phase. The lamellar phase should therefore no longer exist at PEG concentrations above about $c_{\mathrm{p}} = 20$ g/l which is consistent with the experimentally determined phase behaviour shown in Figure 1.

An enhanced attractive contribution to the interactions between the bilayers induced by the polymer could have two possible origins. If the polymer does not adsorb onto the bilayers a depletion interaction could result. On the other hand, a bridging interaction would be possible if the polymer adsorbs onto the bilayers and $d - \delta \approx R_{\mathrm{g}}$.

The former case has been studied by Ligoure *et al.* who derived an expression for the effect of depletion of non-adsorbing polymer on the layer compressibility modulus $\bar{B}^{\mathrm{Pol}}$ [12]. It should also be noted that depletion attraction between two coated surfaces with lipid bilayers (DPPE/DMPC) interacting across a water-PEG mixture has been observed by Kuhl *et al.* [60]. However, in Figure 7 the dashed and plain lines correspond both to the expected behaviours in the case of depletion of non-adsorbing polymer according to Ligoure and co-workers [12] (the dashed line for; $c_{\mathrm{p}} \ll c^*$ and $d - \delta \gg R_{\mathrm{g}}$, the plain line when: $c_{\mathrm{p}} \ll c^*$ and $d - \delta \ll R_{\mathrm{g}}$). Clearly, the depletion model does not describe the experimental results. A possible discrepancy may come about since, in the present work, $2R_{\mathrm{g}} \approx d - \delta$ which is outside the asymptotic limits, $d-\delta \gg R_{\mathrm{g}}$ or $d-\delta \ll R_{\mathrm{g}}$, studied by Ligoure *et al.* Then a straightforward comparison between Ligoure's model and a depletion mechanism in such a regime may not be valid. Moreover, the ion concentration in the vicinity of the bilayer surface should be very high (about 1 M) which may, in turn, affect the PEG solubility close to the membranes enhancing the depletion effect.

Nevertheless, depletion mechanism seems to be unlikely. According to Ficheux *et al.* [13,14], PEG macromolecules adsorb on SDS/octanol bilayer surface. It is most likely that PEG behaves similarly in the present SDS/pentanol system, differing, perhaps, in the total amount of PEG monomers adsorbed. Therefore no depletion interaction can act between the bilayers. The lamellar phase of the SDS/pentanol/water-PEG system can be pictured as a stack of SDS/pentanol bilayers separated by water, with PEG macromolecules weakly anchored on the surface of the membranes. In this case a bridging mechanism could act since the distance between two neighboring bilayers in the lamellar phase (63-60 Å) is very similar to the size of the polymer macromolecules ($2R_{\mathrm{g}} \approx 60$ Å). One can imagine that different segments of a single PEG macromolecule are anchored onto the surface of adjacent SDS/pentanol bilayers leading to their bridging. Unfortunately, there is no model available to describe the evolution of a bridging interaction between two plates as a function of the bulk polymer concentration and hence no quantitative comparison to the experimental data is possible for now.

2) The discussion above assumes that the PEG concentration does not have a strong effect on the nature of the repulsive electrostatic interaction between the bilayers. That is the electrostatic interaction between the bilayers is always given by equation (1). However, PEG might influence the total inter-membrane interaction by altering this *classical* electrostatic interaction. For instance, when PEG adsorbs to the membrane surface the charge distribution could change giving rise to an inhomogeneous surface charge distribution. This, in turn, might modify the electrostatic interactions between SDS/pentanol bilayers that should no longer be described by equation (1). Indeed, independent measurements (to be published elsewhere [61]) show that the double layer repulsion between adsorbed SDS layers onto two opposite hydrophobically modified macroscopic surfaces was decreased upon addition of PEG polymers in water. Comparison between the latter observation and the effect of PEG on electrostatic interaction between bilayers in a lamellar phase is not

straightforward; nevertheless, this could provide another mechanism by which the presence of PEG induces a decrease in $\bar{B}$. However, any theoretical model does not describe such an effect. Hence, no quantitative comparison to the experimental data was possible.

5 Conclusion

The SFA has been shown to be a useful tool for the characterisation of the elastic properties of lamellar phases in several detailed studies [27,28,30]. Some technical difficulties are associated with these measurements with the consequence that only lamellar phases that are not too viscous nor optically turbid can be investigated. In this study, such problems were overcome by working with a bulk micellar phase close to the micellar to lamellar phase transition. Confinement of such a fluid between two smooth rigid walls resulted in a phase transition to a lamellar phase that was stable as long as the confining field was maintained.

The elastic properties of the induced lamellar phase were therefore accessible by direct force measurement allowing an investigation of the effect of added PEG on this system. The measurement of the modulus of layers compression clearly indicated a softening of the repulsive inter-bilayer interactions as the amount of PEG in solvent increased. The SFA results therefore agreed with the bulk phase observations which showed that the addition of PEG favours the micellar phase over the lamellar phase. Ficheux *et al.* arrived at the same conclusions for a similar system [13,14]. The underlying mechanism responsible for the enhancement of the softening of the repulsive inter-membrane interaction was discussed in terms of depletion, bridging effects and modification of the *natural* electrostatic interaction between bilayers. Although the depletion model of Ligoure *et al.* did not fit the experimental results, the depletion mechanism could not be entirely ruled out since the system used here ($2R_g \approx d - \delta$) falls outside the limits of validity of the model. Some improvements to the theoretical model for systems outside the asymptotic regimes would allow for more definitive conclusions. Nevertheless, depletion mechanism is most unlikely since PEG, probably, adsorbs at SDS/pentanol interface. Rather, a bridging mechanism would be more likely since the used polymer is comparable in size to the reticular spacing of the lamellar phase, d. Unfortunately, there is as yet no model to describe the evolution of a bridging interaction between two plates as a function of the bulk polymer concentration. A further test of the bridging mechanism would however be possible by performing similar experiments with polymers of smaller size compared to the distance between two bilayers, $d-\delta$. Finally, the effect of PEG on the electrostatic repulsive interaction between SDS/pentanol bilayers in lamellar phases was considered. Some preliminary measurements, which will be published elsewhere, indicate that this may indeed be significant [61] but, unfortunately, we could not conclude due to the lack of theoretical models. A superimposition of this effect with the bridging mechanism could indeed be operating.

As a final comment we note that the confinement induced micellar to lamellar transition observed in this study, although interesting in itself, was not studied systematically since the main interest here was to determine the effect of a polymer in the lamellar phase. The transition is yet another example of a confinement induced ordering transition and outlines the general importance of the perturbation of a fluid's bulk state by the introduction of an interface of different symmetry. The transition allowed the evolution of the interfacial tension between the micellar phase and the lamellar phase as function of PEG concentration to be estimated. According to these results, it seems that the interfacial tension between the micellar phase and the lamellar phase decreases as the PEG concentration in solvent increases. Nevertheless, both more experimental data and theoretical models are required to confirm and understand this behaviour.

The authors would like to thank M.-F. Ficheux and F. Nallet for providing invaluable information on this system. We are very grateful to Isabelle Javierre for performing the X-ray experiments. We also thank D. Roux, G. Porte, C. Ligoure, J.-F. Joanny, A. Johner and B.W. Ninham for their useful comments and discussions on this work.

References

1. E.D. Goddard, in *Interactions of surfactants with polymers and proteins*, edited by E.D. Goddard, K.P. Ananthapadmanabhan (CRC Press, Boca Raton, Florida, 1993).
2. E.D. Goddard, Colloids Surf. **19**, 255 (1986).
3. E. Ewans, D. Needham, in *Molecular Mechanisms of Membrane Fusion*, edited by S. Ohki, D. Doyle, T.D. Flanagan, S.W. Hui, E. Mayhew (Plenum Press, New York, 1988).
4. T. Nylander, B. Ericsson, Interactions between Proteins and Polar Lipids, in *Food Emulsions*, edited by S.E. Friberg, K. Larsson (Marcel Dekker, New York, Third Edition, 1997).
5. L.T. Boni, S.W. Hui, in *Cell Fusion*, edited by A. Sowers (Plenum Press, New York, 1987).
6. K. Arnold, L. Pratsch, K. Gawrisch, Biochim. Biophys. Acta **728**, 121 (1983).
7. P. Kékicheff, B. Cabane, M. Rawiso, J. Colloid Interface Sci. **102**, 51 (1984).
8. I. Illiopoulos, U. Olsson, J. Phys. Chem. **98**, 1500 (1994).
9. E.Z. Radlinska, T. Gulik-Krzywicki, F. Lafuma, D. Langevin, W. Urbach, C.E. Williams, R. Ober, Phys. Rev. Lett. **74**, 4237 (1995).
10. M. Shing, P. Ober, M. Kléman, J. Phys. Chem. **97**, 11108 (1993).
11. C. Ligoure, G. Bouglet, G. Porte, Phys. Rev. Lett. **71**, 3600 (1993).
12. C. Ligoure, G. Bouglet, G. Porte, O. Diat, J. Phys. II France **7**, 473 (1997).
13. M.-F. Ficheux, A.-M. Bellocq, F. Nallet, J. Phys. II France **5**, 823 (1995).
14. M.-F. Ficheux, Ph.D. thesis, *Étude des systèmes mixtes polymères/tensioactifs en phases organisées : diagrammes*

de phases et interactions, University of Bordeaux I, France, 1995.
15. M.-F. Ficheux, A.-M. Bellocq, F. Nallet, Colloid Surf. A **123**, 253 (1997).
16. B. Demé, V. Dubois, T. Zemb, B. Cabane, J. Phys. Chem. **100**, 3828 (1996).
17. H. Bagger-Jörgensen, U. Olsson, I. Illiapoulos, Langmuir **11**, 1934 (1995).
18. H. Bagger-Jörgensen, Ph.D. thesis, *Polymer Effects on Microemulsions and Lamellar Phases*, Lund University, Sweden, 1997.
19. K. Zang, P. Linse, J. Phys. Chem. **99**, 9130 (1995).
20. E.Z. Radlinska, T. Gulik-Krzywicki, F. Lafuma, D. Langevin, W. Urbach, C.E. Williams, J. Phys. II France **7**, 1393 (1997).
21. D. Roux, C.R. Safinya, F. Nallet, Lamellar phases, in *Micelles, Membranes, Microemulsions and Monolayers*, edited by W.M. Gelbart, A. Ben-Shaul, D. Roux (Springer, New York, 1994).
22. P.-G. de Gennes, J. Phys. Chem **94**, 8407 (1990).
23. J.T. Brooks, C.M. Marques, M.E. Cates, J. Phys. II France **1**, 673 (1991).
24. J.T. Brooks, M.E. Cates, J. Chem. Phys. **99**, 5467 (1993).
25. F. Nallet, D. Roux, J. Prost, J. Phys. France **50**, 3147 (1989).
26. E. Freyssingeas, F. Nallet, D. Roux, Langmuir **12**, 6028 (1996).
27. P. Richetti, P. Kékicheff, J.L. Parker, B.W. Ninham, Nature **346**, 252 (1990).
28. P. Kékicheff, P. Richetti, H.K. Christenson, Langmuir **7**, 1874 (1991).
29. P. Richetti, P. Kékicheff, P. Barois, J. Phys. II France **5**, 1129 (1995).
30. D. Antelmi, P. Kékicheff, J. Phys. Chem. B **101**, 8169 (1997).
31. V.A. Parsegian, R.P. Rand, N.L. Fuller, J. Phys. Chem. **95**, 4777 (1991).
32. H. Bagger-Jörgensen, U. Olsson, Langmuir **12**, 4057 (1996).
33. B. Cabane, R. Duplessix, J. Phys. France **43**, 1529 (1982).
34. B. Cabane, R. Duplessix, J. Phys. France **48**, 651 (1987).
35. R. Zana, P. Lianos, J. Lang, J. Phys. Chem. **89**, 41 (1985).
36. J. Israelachvili, G.E. Adams, Nature **262**, 774 (1976).
37. J.L. Parker, H.K. Christenson, B.W. Ninham, Rev. Sci. Instrum. **60**, 3135 (1989).
38. J.N. Israelachvili, J. Colloid Interface Sci. **44**, 259 (1973).
39. V.E. Shubin, P. Kékicheff, J. Colloid Interface Sci. **155**, 108 (1993).
40. D. Antelmi, P. Kékicheff, P. Richetti, J. Phys. II France **5**, 103 (1995).
41. R.G. Horn, D.T. Smith, W. Haller, Chem. Phys. Lett. **162**, 404 (1989).
42. R.G. Horn, D.T. Smith, Appl. Opt. **30**, 59 (1991).
43. C. Vinches, C. Coulon, D. Roux, J. Phys. II France **4**, 1165 (1994).
44. E. Freyssingeas, D. Roux, F. Nallet, J. Phys.-Cond. Matter **8**, 2801 (1996).
45. P. Richetti, P. Kékicheff, Phys. Rev. Lett. **68**, 1951 (1992).
46. P. Petrov, U. Olsson, H.K. Christenson, S. Miklavic, H. Wennerström, Langmuir **10**, 988 (1994).
47. P. Petrov, S. Miklavic, U. Olsson, H. Wennerström, Langmuir **11**, 3928 (1995).
48. P. Petrov, U. Olsson, H. Wennerström, Langmuir **13**, 3331 (1997).
49. L. Biensan (Moreau), Ph.D. thesis, *Étude des interactions spécifiques entre deux surfaces près d'une transition de phase*, University of Bordeaux I, France, 1996.
50. S.T. Milner, D.C. Morse, Phys. Rev. E **54**, 3793 (1996).
51. L.R. Fisher, J.N. Israelachvili, Colloids Surf. **3**, 303 (1981).
52. E.J. Wanless, H.K. Christenson, J. Chem. Phys. **101**, 4260 (1994).
53. H.K. Christenson, Phys. Rev. Lett. **73**, 1821 (1994).
54. J. Crassous, E. Charlaix, J.L. Loubet, Europhys. Lett. **28**, 37 (1994).
55. C. Quillet, C. Blanc, M. Kléman, Phys. Rev. Lett. **77**, 522 (1996).
56. H.K. Christenson, J. Colloid Interface Sci. **104**, 234 (1985).
57. D. Antelmi, Ph.D. thesis, *The confinement induced sponge to lamellar transformation*, Australian National University, Canberra, Australia, 1996.
58. D. Roux, C.R. Safinya, J. Phys. France **49**, 307 (1988).
59. F. Nallet, D. Roux, C. Quillet, P. Fabre, S.T. Milner, J. Phys. France II **4**, 1477 (1994).
60. T. Kuhl, Y. Guo, J.L. Alderfer, A.D. Berman, D. Leckband, J. Israelachvili, S. Hui, Langmuir **12**, 3003 (1996).
61. P. Kékicheff and co-workers, unpublished results.